ChemPubSoc Europe

DOI: 10.1002/open.201700115

Open Access ChemistryOPEN Full Papers

Quantitative Structure–Retention Relationships for Polycyclic Aromatic Hydrocarbons and their Oligoalkynyl-Substituted Derivatives

Gaël Rouillé,[a] Cornelia Jäger,*[a] Friedrich Huisken,[a] Thomas Henning,[b] Regina Czerwonka,[c] Gabriele Theumer,[c] Carsten Börger,[c] Ingmar Bauer,[c] and Hans-Joachim Knölker*[c]

Reversed-phase high-performance liquid chromatography (RP-HPLC) has been carried out for a series of unsubstituted polycyclic aromatic hydrocarbons (PAHs) and the corresponding ethynyl, 1,3-butadiynyl, and 1,3,5-hexatriynyl derivatives. Theoretical values of the isotropic polarizability and several polarity descriptors have been computed for each compound by using semiempirical models and density functional theory (DFT), with the aim of evaluating linear functions as quantitative structure–retention relationships (QSRRs). The polarity has been described by using either the permanent electric dipole moment, the subpolarity, or a topological electronic index. Three types of partial atomic charges have been used to calculate the subpolarity and a topological index. The choice of the theoretical model, of the polarity descriptor, and of the partial atomic charges is discussed and the resulting QSRRs are compared. Calculating the retention times from the polarizability and the topological electronic index (AM1, PM3, or DFT-B3LYP/6–31+G(d,p)) gives the best agreement with the experimental values.

1. Introduction

Polycyclic aromatic hydrocarbons (PAHs) are a focus of current research because of their electronic, optical, structural, and self-organizing properties and thus are interesting materials for nanotechnologies. Our interest in these compounds derives from the fact that PAHs constitute one of the most abundant families of molecules in interstellar space.[1] They are formed in carbon-rich stars by chemical reactions that also take place in combustion processes on earth.[2] Most likely, ethynyl derivatives are intermediates in the formation and growth processes of PAHs, and oligoalkynyl derivatives may also be involved. For example, ethynylbenzene, diethynylbenzene, ethynylnaphthalene, and butadiynylbenzene were identified in the combustion process of small hydrocarbons.[3,4] Several ethynyl-substituted PAHs were also found in the combustion of primary tar,[5] and as products of the pyrolysis of catechol,[6] the dominating phenol in tobacco smoke.

In a recent article, we presented the UV/Vis spectra of Ne matrix-isolated ethynyl- and 1,3-butadiynyl-substituted PAHs.[7] We also recorded the IR spectra of these compounds embedded in CsI pellets.[7] Subsequently, we measured the UV/Vis spectrum of Ne matrix-isolated 9,10-diethynylanthracene.[8] These studies prompted us to investigate butadiynyl- and hexatriynyl-substituted PAHs by reversed-phase high-performance liquid chromatography (RP-HPLC) for the determination of their experimental retention data. Our experimental data are useful for the identification of these compounds in samples analyzed by RP-HPLC and offer the possibility to establish quantitative structure–retention relationships (QSRRs).[9] Retention values are the retention time, the retention index, and the retention factor (also called capacity factor). The mechanism of retention in RP-HPLC is widely described in terms of partition and adsorption, which denote the positioning of the retained analyte in relation to the alkyl chains of the stationary phase.[10,11] Modeling of these processes is complex because various interactions are involved in a system that comprises the analyte molecules, the alkyl chains of the stationary phase, and also the solvent molecules of the mobile phase.[12] Although linear solvation energy relationships represent a general approach to modeling retention,[13] the parameters required to describe the analytes as solutes are often not readily available.

[a] Dr. G. Rouillé, Dr. C. Jäger, Prof. Dr. F. Huisken
Laboratory Astrophysics Group of the Max Planck Institute for Astronomy at the Friedrich Schiller University Jena
Institute of Solid State Physics
Helmholtzweg 3, 07743 Jena (Germany)
E-mail: cornelia.jaeger@uni-jena.de

[b] Prof. Dr. T. Henning
Max Planck Institute for Astronomy
Königstuhl 17, 69117 Heidelberg (Germany)

[c] R. Czerwonka, G. Theumer, Dr. C. Börger, Dr. I. Bauer, Prof. Dr. H.-J. Knölker
Department Chemie, Technische Universität Dresden
Bergstrasse 66, 01069 Dresden (Germany)
E-mail: hans-joachim.knoelker@tu-dresden.de

Supporting Information and the ORCID identification number(s) for the author(s) of this article can be found under https://doi.org/10.1002/open.201700115.

On the other hand, structure-related molecular properties can be computed easily and simple functions of these descriptors can predict retention values despite the complexity of the phenomenon. Examples of descriptors employed in the QSRRs of PAHs are the number of carbon atoms,[14] connectivity indices,[15] molecular sizes,[16] the moment of inertia,[17] and the quadrupole moment together with the polarizability.[18]

We analyzed retention data obtained for the unsubstituted, ethynyl-, butadiynyl-, and hexatriynyl-substituted PAHs. In an earlier work, Ledesma and Wornat studied a series of unsubstituted and ethynyl-substituted PAHs.[19] To establish QSRRs, we investigated the linear relationships of the retention times for the compounds **1**–**4** with the polarizability and polarity descriptors derived from theoretical calculations (Figure 1).

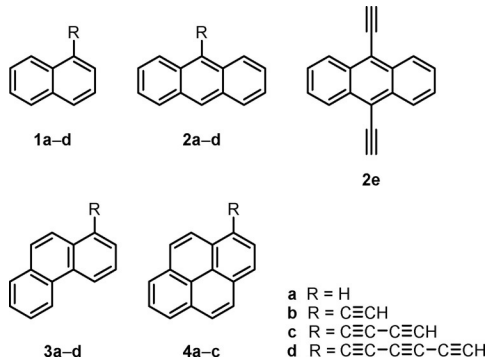

Figure 1. Structures of the polycyclic aromatic hydrocarbons (PAHs) **1**–**4**.

2. Results and Discussion

2.1. Retention Time

The experimentally observed total retention times t_R and the corresponding retention factors k of the compounds **1**–**4** obtained by RP-HPLC are given in Table 1. As expected, t_R increases with the number of carbon atoms present in the molecule.[14] The corresponding chromatograms confirm the purity of the samples (Figure S1, Supporting Information).

Table 1. Total retention times t_R and retention factors k of the PAHs **1**–**4**.

Compound	Formula	t_R [min]	k[a]
1a	$C_{10}H_8$	7.23	3.58
1b	$C_{12}H_8$	8.33	4.27
1c	$C_{14}H_8$	11.73	6.42
1d	$C_{16}H_8$	15.80	9.00
2a	$C_{14}H_{10}$	12.89	7.16
2b	$C_{16}H_{10}$	13.57	7.59
2c	$C_{18}H_{10}$	15.96	9.10
2d	$C_{20}H_{10}$	19.36	11.25
2e	$C_{18}H_{10}$	15.41	8.75
3a	$C_{14}H_{10}$	11.92	6.54
3b	$C_{16}H_{10}$	13.25	7.39
3c	$C_{18}H_{10}$	16.18	9.24
3d	$C_{20}H_{10}$	20.20	11.78
4a	$C_{16}H_{10}$	14.60	8.24
4b	$C_{18}H_{10}$	16.38	9.37
4c	$C_{20}H_{10}$	19.54	11.37

[a] Retention factor: $k=(t_R-t_M)/t_M$. Hold-up time: t_M estimated to be 1.58 min.

2.2. Molecular Descriptors

Ledesma and Wornat established QSRRs for PAHs and their ethynyl derivatives by using several molecular descriptors,[19] which are the principal moment of inertia, the total energy, the isotropic polarizability α, the ionization potential, the permanent electric dipole moment μ, and the quantum chemical submolecular polarity Δ (also called the subpolarity parameter).[19–21] Based on that study, we focused on α, μ, Δ, and, additionally, on the topological index T^E.[22] All these descriptors are related to electrostatic properties and consequently to intermolecular potential energies. As the physical values of the descriptors are in most of the cases not known, the establishment of QSRRs requires theoretical values that can be computed by application of various methods. We have calculated the descriptors by using the semiempirical AM1,[23] PM3,[24] PM6,[25] and PM7[26] models. In addition, we have applied two DFT-based programs. In the course of our previous work on polyynyl-substituted PAHs,[7] the widely used B3LYP hybrid functional[27–29] was employed in combination with the cc-pVTZ basis set.[30–32] This combination has been used again in the present study. Further results have been obtained by applying the B3LYP functional in combination with the 6–31+G(d,p) basis set.[33]

2.3. Polarizability

Theoretical values of the polarizability α have been compared with experimental values reported in the literature for the unsubstituted PAHs (Table S1 in the Supporting Information). The values obtained directly with the AM1, PM3, and PM6 models, using any version of the Gaussian software or early versions of MOPAC, are strongly underestimated. The 2012 version of the MOPAC program[34] includes a correction for the computation of the polarizability [Eq. (1)]:

$$\alpha^{(\text{corrected})} = a + C_1\alpha^{(\text{direct})} + C_C n_C + C_H n_H \quad (1)$$

n_C: number of carbon atoms in the molecule; n_H: number of hydrogen atoms; a, C_1, C_C, C_H: numerical parameters specific to each model.[34]

Linear regressions showed that the polarizabilities obtained from the corrected semiempirical PM6 and PM7 models and the DFT-based calculations are in better agreement with the experimental values for the unsubstituted molecules.[35–37] According to previous reports, the PM6 model provided better results than AM1 and PM3 for PAHs and fullerenes.[38] Still, the best results have been obtained with the DFT-B3LYP/6–31+G(d,p) approach. Although the 6–31+G(d,p) basis set is smaller than the cc-pVTZ basis set, it comprises diffuse functions, which are known to improve the results of various calculations including the determination of polarizabilities.[39]

Lacking experimental values for the substituted molecules, we use the results obtained from the DFT-B3LYP/6–31+G(d,p)

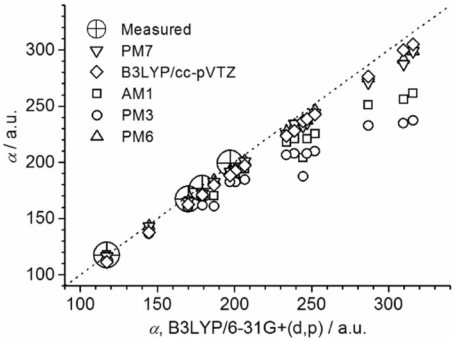

Figure 2. Theoretical values of the isotropic molecular polarizability α for compounds **1a**–**4c** computed by various models compared with those obtained at the B3LYP/6–31+G(d,p) level of theory (graphical presentation of the values from Table S1 in the Supporting Information).

approach as a reference to visualize possible differences between the polarizabilities computed by various models. Figure 2 shows that the PM6, PM7, DFT-B3LYP/cc-pVTZ, and DFT-B3LYP/6–31+G(d,p) approaches provide similar values for the polarizability. In contrast, the AM1 and PM3 models give values that deviate with increasing length of the polyynyl side chain. These results confirm that the values for the polarizability of the polyynyl-substituted PAHs obtained from the AM1 and PM3 models are not reliable even with the correction applied in MOPAC 2012 (see above). Their use in QSRRs should be avoided in favor of the values computed with the more recent PM6 and PM7 models or with the DFT approaches.

2.4. Electric Dipole Moment

The theoretical values for the permanent electric dipole moment μ of the substituted PAHs have been calculated by using semiempirical models and DFT (Table S2 in the Supporting Information). For the structurally related phenylacetylene, an experimental value for μ is available and thus could be compared with the theoretical value.[40] Among the unsubstituted PAHs, only compound **3a** has a non-centrosymmetric structure and thus a permanent electric dipole moment. However, its magnitude is negligible.[41] As observed for the polarizability of unsubstituted PAHs, the permanent electric dipole moment of phenylacetylene is better estimated by using the DFT-based methods and the PM6 and PM7 models. Our DFT calculations overestimate μ by approximately 10%, whereas the PM6 and PM7 models underestimate the value by about 10% and 20%, respectively. The values derived from the AM1 and PM3 models are 60% and 75% too low. Thus, the values of electric dipole moments computed with the PM6 and PM7 models or DFT-based methods should be used for QSRRs.

2.5. Submolecular Polarity

In Ledesma and Wornat's study of PAHs and their ethynyl derivatives,[19] the most accurate QSRRs were obtained by combining the polarizability α and the submolecular polarity Δ calculated by AM1. The submolecular polarity, or subpolarity, corresponds to the largest difference in partial charge for two bound atoms. It considers the role of local electric dipoles of an analyte and its interaction with the molecules of the mobile and stationary phases.[20] The subpolarity is a more realistic indicator of molecular polarity than the electric dipole moment. The overall dipole moment μ does not provide information on local dipoles of a molecule. For example, the value of μ for a centrosymmetric molecule is zero, irrespective of local dipole moments.

The position of the polarity-defining bond in the molecular structure has not been considered for the determination of the subpolarity Δ. However, the exposure of this bond to solvent molecules, which depends on steric effects, is crucial. The concept of subpolarity has limitations because partial atomic charges can be determined by various methods. For instance, the so-called Mulliken charges can vary significantly and fail to describe the ionic or covalent nature of a bond, as in the case of hydrocarbons.[42,43] Regarding other methods, partial charges derived from the atomic polar tensors (APTs) appear satisfactory.[43] The CHELPG (CHarges from ELectrostatic Potentials using a Grid-based method) scheme determines partial charges in accordance with the value for the electrostatic potential at selected locations of the molecule.[44–46]

Subpolarity values have been calculated by using the partial charges derived from the self-consistent field electronic density (Tables S3 and S4 in the Supporting Information). Mulliken and atomic polar tensor charges and subpolarities have been computed by using a range of theoretical models. Subpolarities obtained from the CHELPG charges are added for the B3LYP/6–31+G(d,p) approach. All partial charges were obtained by using the Gaussian software except for those derived with the PM7 model. The PM7 Mulliken charges were computed with MOPAC 2012 (Coulson charges computed with MOPAC have been taken into account as they are equivalent to the Mulliken charges calculated with Gaussian).

Figure 3 represents the electrostatic potential V of anthracene (**2a**) and its derivatives **2b**–**e** at an electronic isodensity surface obtained at the B3LYP/6–31+G(d,p) level of theory from the self-consistent field full density matrix. The largest difference of potential is observed at the acetylenic C–H bond. The same calculation carried out for the compounds **1**, **3**, and **4** shows that this result applies to all polyynyl derivatives (Figure S2 in the Supporting Information). A slight increase for the maximum value of the electrostatic potential is observed with increasing length of the side chain. In the unsubstituted PAHs, aromatic C–H bonds are the sites of the largest potential differences. Their maximum values are significantly lower than those obtained for the polyynyl-substituted PAHs.

The Mulliken subpolarities Δ_{MULL} (see Table S3 in the Supporting Information) obtained from the semiempirical models are not overestimated as they are below 0.5 e. For all substituted compounds, the most polar bond is the acetylenic C–H bond, irrespective of the semiempirical model employed. This observation is in agreement with the electrostatic potentials computed at the DFT level. Thus, the value of the subpolarity essentially reflects the absence ($\Delta_{MULL} \approx 0.20$–$0.35$ e) or presence ($\Delta_{MULL} \approx 0.33$–$0.43$ e) of a PAH polyynyl side chain. The subpolarity decreases slightly for longer side chains, whereas

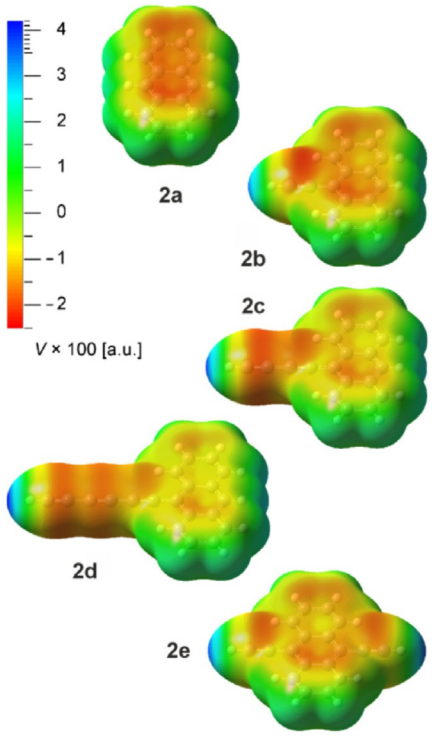

Figure 3. Values of the theoretical electrostatic potential *V* mapped on an electronic isodensity (4×10^{-4} a.u.) surface as obtained at the B3LYP/6–31+G(d,p) level of theory for anthracene (**2a**) and its derivatives **2b**–**e**.

the electric dipole moment increases steadily with the length of the side chain (Tables S2 and S3 in the Supporting Information). The inverse behavior of the two polarity descriptors is rationalized by the fact that the subpolarity Δ relates to a local polarity whereas the electric dipole moment μ represents the overall polarity of the molecules.

The Mulliken subpolarity of the non-substituted and ethynyl-substituted molecules computed at the DFT-B3LYP/cc-pVTZ level provides values in the same order of magnitude as those obtained with the semiempirical models. However, in contrast to the results with the semiempirical models, the values for the subpolarity increase with the size of the polyynyl group up to ≈0.88 e for the hexatriynyl-substituted species. At the DFT-B3LYP/6–31+G(d,p) level of theory, the subpolarity computed by using the Mulliken charges provides overestimated values up to ≈2.6 e.

The subpolarity calculated by using the APT charges reaches a value of almost 0.9 e at the B3LYP/6–31+G(d,p) level of theory (Table S4 in the Supporting Information). The values derived from the semiempirical models reach up to ≈0.77 e. They indicate the absence (Δ_{APT}≈0.19–0.45 e) or presence (Δ_{APT}≈0.54–0.77 e) of an acetylenic side chain. Thus, the subpolarity is an adequate molecular descriptor if the molecule has a unique bond, significantly more polar than all others.

2.6. Topological Electronic Index

By using semiempirical models, the topological index calculated with Mulliken charges (T^E_{MULL}) is higher for substituted PAHs than for the corresponding unsubstituted molecules (Table S5 in the Supporting Information). With the AM1 and PM3 models, T^E_{MULL} becomes substantially larger for the 9,10-diethynylanthracene (**2e**) than for the mono-substituted anthracenes **2b**–**d**. Thus, in contrast to the subpolarity Δ_{MULL}, the index T^E_{MULL} is sensitive to the number of acetylenic C–H bonds.

Table S6 (in the Supporting Information) presents values of the topological index calculated with APT and CHELPG charges, T^E_{APT} and T^E_{CHELPG}, respectively. The trend for the value of T^E_{APT} within a series of substituted PAHs is independent of the theoretical model used for the relevant charges (Table S6 in the Supporting Information). T^E_{APT} increases with the length of the side chain. Using all models, the value of T^E_{APT} for **2e** is larger than for **2c**, and using the AM1 and PM3 models it is also larger than for **2d**. The values of T^E_{APT} as a function of substitution follow the same trend as the electrostatic potentials calculated with DFT, whereas the values of T^E_{CHELPG} computed by using the B3LYP/6–31+G(d,p) model do not.

2.7. Resulting Quantitative Structure–Retention Relationships

We have established QSRRs by correlating linear functions of two variables, the polarizability α and one of the polarity descriptors (μ, Δ, or T^E), to the observed retention times t_R (Table S7 in the Supporting Information). Parameters describing the quality of the regression for t_R are also presented in Table S7. In agreement with Ledesma and Wornat's finding,[19] our results show that the linear functions of polarizability and polarity in all cases correlate well with the total retention time: $r>0.97$. None of the regressions using μ as the polarity descriptor give the best correlations. In contrast, all regressions using T^E_{APT} as polarity descriptor provide excellent correlations (except for application of the PM6 semiempirical model). The correlations of the regressions using Δ_{MULL}, Δ_{APT}, or T^E_{MULL} as polarity descriptors are good when computed with AM1 and PM3, but only moderate when PM6, PM7, and DFT are applied. The moderate correlations when using μ and the generally excellent correlations using T^E_{APT} support the hypothesis that local electric dipoles must appear in the description of the polarity and thus play a role in the retention process. For example, the retention times t_R calculated with DFT at the B3LYP/6–31+G(d,p) level when using T^E_{APT} as polarity descriptor show a very good agreement (correlation coefficient: $r=0.990$) with the experimental values (Figure 4, Table S8 in the Supporting Information). Irrespective of the polarity descriptor that is applied (Δ_{MULL}, Δ_{APT}, T^E_{MULL}, or T^E_{APT}), the older semiempirical models AM1 and PM3 provide better results compared with PM6 and PM7.

In the QSRRs, the sign of the coefficient for each descriptor provides information on the interactions governing the retention behavior. In all QSRRs, the coefficient for the polarizability α is positive, indicating that PAH molecules with larger polarizabilities are eluted more slowly. In comparison, the sign of the coefficient for the polarity descriptor (μ, Δ, or T^E) varies. For a given polarizability α and a negative coefficient for the polarity descriptor, a higher polarity leads to a faster elution, as con-

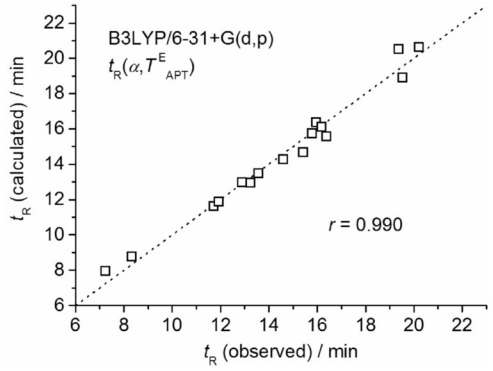

Figure 4. Calculated retention times (t_R) compared with the observed values. The retention times were calculated by using the theoretical polarizabilities α and the topological electronic index values T^E_{APT} with the B3LYP/6–31+G(d,p) method (graphical presentation of the values from Table S8 in the Supporting Information).

firmed, for example, by the isomers of the formula $C_{16}H_{10}$: compounds **2b**, **3b**, and **4a** (Table S8 in the Supporting Information).

3. Conclusions

We successfully performed RP-HPLC for a series of PAHs consisting of the parent compounds as well as ethynyl, 1,3-butadiynyl, and 1,3,5-hexatriynyl derivatives. We have investigated the dependency of their retention times as a linear function of the polarizability α and polarity descriptors μ, Δ, and T^E for QSRRs. The best results were obtained by calculating either α and T^E by using DFT at the B3LYP/6–31+G(d,p) level or by calculating α, Δ, and T^E values with the AM1 and PM3 models. Finally, the most reliable QSRRs, resulting from the present gradient-elution RP-HPLC data, shows a linear correlation of the retention time t_R with the isotropic polarizability α and the polarity T^E. In conclusion, the present results may be applicable for calculating the retention times of structurally related (oligo)alkynyl-substituted arenes. Moreover, the data could be useful for the identification of these compounds in environmental samples.

Experimental Section

Chemical Reagents

The substances included in our study are the unsubstituted PAHs naphthalene (**1a**), anthracene (**2a**), phenanthrene (**3a**), and pyrene (**4a**). The ethynyl derivatives are 1-ethynylnaphthalene (**1b**), 9-ethynylanthracene (**2b**), 9,10-diethynylanthracene (**2e**), 9-ethynylphenanthrene (**3b**), and 1-ethynylpyrene (**4b**). The butadiynyl-substituted species are 1-butadiynylnaphthalene (**1c**), 9-butadiynylanthracene (**2c**), 9-butadiynylphenanthrene (**3c**), and 1-butadiynylpyrene (**4c**). Finally, the hexatriynyl derivatives are 1-hexatriynylnaphthalene (**1d**), 9-hexatriynylanthracene (**2d**), and 9-hexatriynylphenanthrene (**3d**). The structures of the substances are depicted in Figure 1.

The unsubstituted PAHs as well as compounds **1b** and **3b** were purchased from Sigma–Aldrich whereas **4b** was purchased from ABCR. Samples of **2b**,[47,48] **2e**,[49–51] **1c**,[52] **1d**,[52,53] **2c**,[54] **2d**,[54] **3c**,[55,56] **3d**,[55,56] and **4c**[57] were prepared by following the approach as shown for the alkynyl-substituted anthracenes (Scheme 1, Supporting Information). Thus, the ethynyl-substituted

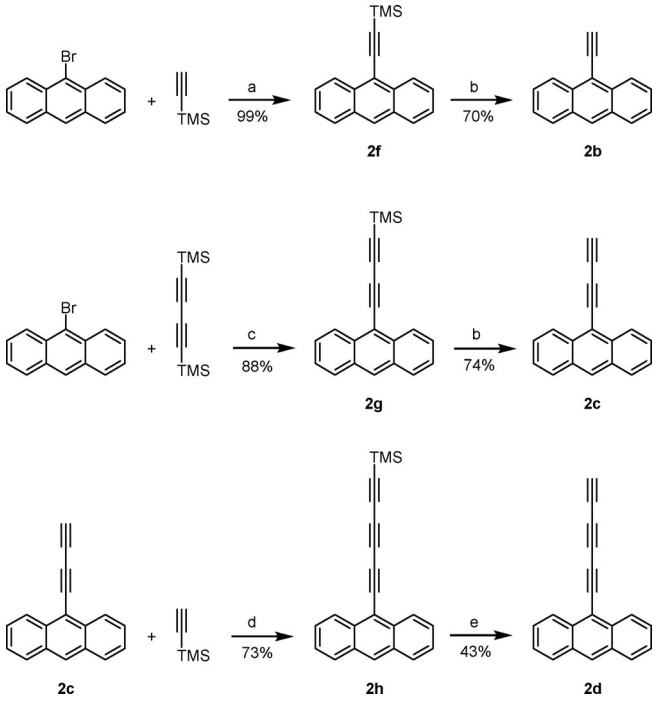

Scheme 1. Reagents and conditions for the synthesis of 9-ethynyl-, 9-butadiynyl-, and 9-hexatriynylanthracenes (**2b**, **2c**, and **2d**). a) Ethynyltrimethylsilane (5.0 equiv), *n*BuLi (5.3 equiv), −78 °C to 0 °C, 30 min, $ZnCl_2$ (5.0 equiv), THF, 0 °C, 3 h, then 9-bromoanthracene (1.0 equiv), 10 mol% $Pd(PPh_3)_4$, THF, reflux, 15 h. b) K_2CO_3 (1.0 equiv), CH_2Cl_2/MeOH, rt, 3 h. c) Bis(trimethylsilyl)butadiyne (10 equiv), *n*BuLi (10 equiv), $ZnCl_2$ (10 equiv), THF, −78 °C to rt, 30 min, then 9-bromoanthracene (1.0 equiv), 5 mol% $Pd(PPh_3)_4$, THF, reflux, 2 d, exclusion of light. d) Ethynyltrimethylsilane (30 equiv), CuCl (15 equiv), CH_2Cl_2, O_2 (1 atm), rt, 2 h, then TMEDA (66 equiv), CH_2Cl_2, O_2 (1 atm), rt, 2 h. e) $AgNO_3$ (2.7 equiv), EtOH/H_2O (3:1), rt, 15 min, then KCN (13 equiv), rt, 15 min, exclusion of light.

anthracenes **2b** and **2e** were obtained by a Negishi-type coupling[58–61] of 9-bromoanthracene or 9,10-dibromoanthracene with ethynyltrimethylsilane (Scheme 1, step a) following a procedure by John and Tour.[62] Subsequent protodesilylation by using K_2CO_3 in methanol provided the free terminal acetylenes (Scheme 1, step b). In our hands, this approach turned out to be more efficient than the Sonogashira–Hagihara protocol,[63] which has been employed by Jäschke et al.[64] and Fallis et al.[65] for the synthesis of **2b**. A Negishi-type reaction of bromoarenes with chloro(trimethylsilylbutadiynyl)zinc, which was generated in situ from bis(trimethylsilyl)butadiyne by treatment with *n*BuLi and zinc chloride, led to the trimethylsilylbutadiynyl-substituted arenes (Scheme 1, step c). This protocol includes a selective monodesilylation of bis(trimethylsilyl)-butadiyne by *n*BuLi. Consequently, we could apply the same conditions for the coupling of bromoarenes with bis(trimethylsilyl)butadiyne as for the coupling with ethynyltrimethylsilane. Monodesilylation of bis(trimethylsilyl)butadiyne and transformation into an alkynylzinc reagent was described earlier by Frauenrath and coworkers by using MeLi·LiBr in Et_2O,[66,67] a reagent frequently applied for the monodesilylation of bis(trimethylsilyl)alkynes.[68–74] The (trimethylsilylbutadiynyl)arenes were protodesilylated by using

K_2CO_3 in methanol. It should be noted that the trimethylsilyl-protected butadiynylarenes are stable and can be handled without special precautions. However, the free butadiynylarenes decompose under the influence of heat and/or light. Therefore, light should be excluded during the synthesis and heating above room temperature has to be avoided. Removal of the solvents was achieved under reduced pressure at 5–10 °C. The synthesis of the hexatriynylarenes **1d**, **2d**, and **3d** was achieved by using an oxidative Glaser–Hay coupling between butadiynylarenes and ethynyltrimethylsilane (Scheme 1, step d).[56,75] Owing to extreme instability, desilylation of the hexatriynylarenes required even milder conditions and was achieved by reaction of the trimethylsilylalkynes with silver nitrate to the corresponding silver alkynylides by following a procedure of Schmidt and Arens.[76] The latter were converted to the free alkynes by addition of a concentrated aqueous solution of potassium cyanide (Scheme 1, step e). The alkynylarenes and their trimethylsilyl-protected precursors have been structurally confirmed by ^{1}H NMR, ^{13}C NMR, IR, mass spectra, and elemental analyses. Owing to the low stability and low solubility, the hexatriynylarenes **1d**, **2d**, and **3d** have been characterized only by ^{1}H NMR spectroscopy. Moreover, whenever possible, the absorption spectra acquired during the RP-HPLC procedure were compared with the corresponding literature data and showed an excellent agreement. Data were found for the unsubstituted PAHs,[77] and for the derivatives **1b**,[77] **1d**,[52] **2b**,[48] **2c**,[54] **2d**,[54] **2e**,[49] **3b**,[55,77] **3c**,[55] **3d**,[55] and **4b**.[77] Figure S1 (in the Supporting Information) shows the chromatograms. The absorption spectra measured during the RP-HPLC procedure are shown in Figure S3 (in the Supporting Information) and the wavelengths of the observed absorptions are reported in Table S9 (in the Supporting Information). The numerical data derived from the ^{1}H NMR, ^{13}C NMR, IR, and mass spectra, and from the elemental analyses are reported in the Supporting Information. The NMR spectra are shown in Figures S4–S52 (Supporting Information).

Instrumentation

The HPLC apparatus was a JASCO system equipped with solvent delivery pumps model PU-2080 Plus and a diode array detector model MD-2010 Plus. The detector covered the wavelengths from 195 to 600 nm. As stationary phase, we used a polymeric C18-type column ReproSil PAH-EPA (Dr. Maisch HPLC GmbH), with grain size of 5 μm, length of 250 mm, and diameter of 4 mm.

Procedure

Mobile phase: MeCN/H_2O. Gradient elution with an initial ratio of MeCN/H_2O = 1:1. After 5 min, the concentration of MeCN was increased linearly to obtain 85% MeCN over a period of 10 min. Then, it was increased further up to a concentration of 100% MeCN after a period of 5 min and was kept at this level. Flow rate: 1 mL min^{-1}. The temperature of the column was maintained at 30 °C. For each substance, the injected volume was 100 μL. The chromatograms were monitored by measuring the absorption at 254 nm with an interval of 0.5 s. Simultaneously, absorption measurements were recorded at all wavelengths from 195 to 600 nm in 1 nm increments (Figure S3, Table S9 in the Supporting Information).

The reproducibility of the RP-HPLC procedure was demonstrated by repeating the t_R measurements (variations of t_R: ≤ 0.03 min). An accurate determination of the hold-up time t_M was not possible, but it can be estimated from the signal caused by the change of the refractive index when the injected mobile phase passes the detector. The time corresponding to the first maximum in the signal varies from 1.442 to 1.658 min in the measurements given in Table 1, with an average value of 1.577 min. Thus, a value of 1.58 min has been estimated for t_M.

Computational Methods

All calculations were performed with the Gaussian 09 software,[78] with the exception of those involving the PM7 semiempirical model, which is not implemented in this version of the software. Care was taken to always employ the predefined ultrafine grid for the computation of integrals. The calculations with the PM7 semiempirical model were carried out with the MOPAC 2012 program.[23] When required, the calculations with the AM1,[23] PM3,[24] and PM6[25] models were run a second time with MOPAC 2012.

For determination of the molecular properties, the following protocol was applied. First, the geometry of the molecule was optimized while imposing the tight and precise convergence criteria implemented in the Gaussian 09 and MOPAC 2012 softwares, respectively. During optimization, the structure was constrained to the relevant symmetry, either C_s, C_{2v}, or D_{2h}. Then, the vibrational modes were calculated to verify that the optimized geometry corresponded to a minimum on the potential energy surface. The values of selected molecular descriptors were calculated by using the same model as for geometry optimization. The calculated descriptors are the isotropic polarizability α, the permanent electric dipole moment μ, the quantum chemical submolecular polarity Δ,[20,21] also called subpolarity,[19] and a topological electronic index T^E.[22]

Acknowledgments

This work was carried out within a collaboration between the Max-Planck-Institut für Astronomie, the Friedrich-Schiller-Universität Jena, and the Technische Universität Dresden. The support of the Deutsche Forschungsgemeinschaft (Hu 474/24) is gratefully acknowledged. Information provided by Prof. Dr. Roman Kaliszan is greatly appreciated. We are thankful to Ms. Gabriele Born of the Friedrich-Schiller-Universität Jena for performing the RP-HPLC measurements.

Conflict of Interest

The authors declare no conflict of interest.

Keywords: alkynes · density functional calculations · liquid chromatography · polycyclic aromatic hydrocarbons · semiempirical calculations

[1] A. G. G. M. Tielens, *Annu. Rev. Astron. Astrophys.* **2008**, *46*, 289–337.
[2] M. Frenklach, E. D. Feigelson, *Astrophys. J.* **1989**, *341*, 372–384.
[3] H. Bockhorn, F. Fetting, H. W. Wenz, *Ber. Bunsenges. Phys. Chem.* **1983**, *87*, 1067–1073.
[4] Y. Carpentier, T. Pino, P. Bréchignac, *J. Phys. Chem. A* **2013**, *117*, 10092–10104.
[5] E. B. Ledesma, M. A. Kalish, M. J. Wornat, P. F. Nelson, J. C. Mackie, *Energy Fuels* **1999**, *13*, 1167–1172.
[6] M. J. Wornat, E. B. Ledesma, N. D. Marsh, *Fuel* **2001**, *80*, 1711–1726.

[7] G. Rouillé, M. Steglich, Y. Carpentier, C. Jäger, F. Huisken, T. Henning, R. Czerwonka, G. Theumer, C. Börger, I. Bauer, H.-J. Knölker, *Astrophys. J.* **2012**, *752*, 25.
[8] G. Rouillé, C. Jäger, F. Huisken, T. Henning, *Proc. Int. Astron. Union* **2013**, *9*, 276 – 280.
[9] R. Kaliszan, *Chem. Rev.* **2007**, *107*, 3212 – 3246.
[10] K. A. Dill, *J. Phys. Chem.* **1987**, *91*, 1980 – 1988.
[11] J. G. Dorsey, K. A. Dill, *Chem. Rev.* **1989**, *89*, 331 – 346.
[12] P. Nikitas, A. Pappa-Louisi, *J. Chromatogr. A* **2009**, *1216*, 1737 – 1755.
[13] M. Vitha, P. W. Carr, *J. Chromatogr. A* **2006**, *1126*, 143 – 194.
[14] R. B. Sleight, *J. Chromatogr.* **1973**, *83*, 31 – 38.
[15] M. J. M. Wells, C. R. Clark, R. M. Patterson, *Anal. Chem.* **1986**, *58*, 1625 – 1633.
[16] M. N. Hasan, P. C. Jurs, *Anal. Chem.* **1983**, *55*, 263 – 269.
[17] E. R. Collantes, W. Tong, W. J. Welsh, *Anal. Chem.* **1996**, *68*, 2038 – 2043.
[18] Q.-H. Wan, L. Ramaley, R. Guy, *Anal. Chem.* **1997**, *69*, 4581 – 4585.
[19] E. B. Ledesma, M. J. Wornat, *Anal. Chem.* **2000**, *72*, 5437 – 5443.
[20] K. Ośmiałowski, J. Halkiewicz, A. Radecki, R. Kaliszan, *J. Chromatogr. A* **1985**, *346*, 53 – 60.
[21] R. Kaliszan, K. Ośmiałowski, S. A. Tomellini, S.-H. Hsu, S. D. Fazio, R. A. Hartwick, *J. Chromatogr. A* **1986**, *352*, 141 – 155.
[22] K. Ośmiałowski, J. Halkiewicz, R. Kaliszan, *J. Chromatogr. A* **1986**, *361*, 63 – 69.
[23] M. J. S. Dewar, E. G. Zoebisch, E. F. Healy, J. J. P. Stewart, *J. Am. Chem. Soc.* **1985**, *107*, 3902 – 3909.
[24] J. J. P. Stewart, *J. Comput. Chem.* **1989**, *10*, 209 – 220.
[25] J. J. P. Stewart, *J. Mol. Model.* **2007**, *13*, 1173 – 1213.
[26] J. J. P. Stewart, *J. Mol. Model.* **2013**, *19*, 1 – 32.
[27] A. D. Becke, *Phys. Rev. A* **1988**, *38*, 3098 – 3100.
[28] C. Lee, W. Yang, R. G. Parr, *Phys. Rev. B* **1988**, *37*, 785 – 789.
[29] A. D. Becke, *J. Chem. Phys.* **1993**, *98*, 5648 – 5652.
[30] T. H. Dunning, *J. Chem. Phys.* **1989**, *90*, 1007 – 1023.
[31] D. E. Woon, T. H. Dunning, *J. Chem. Phys.* **1993**, *98*, 1358 – 1371.
[32] E. R. Davidson, *Chem. Phys. Lett.* **1996**, *260*, 514 – 518.
[33] M. J. Frisch, J. A. Pople, J. S. Binkley, *J. Chem. Phys.* **1984**, *80*, 3265 – 3269.
[34] J. J. P. Stewart, MOPAC2012, Version 12.239W, Stewart Computational Chemistry, Colorado Springs, CO, USA, **2012**.
[35] J. Schuyer, L. Blom, D. W. Krevelen, *Trans. Faraday Soc.* **1953**, *49*, 1391 – 1401.
[36] R. J. W. Le Fèvre, K. M. S. Sundaram, *J. Chem. Soc.* **1963**, 4442 – 4446.
[37] M. F. Vuks, *Opt. Spectrosc.* **1966**, *20*, 361 – 364.
[38] A. Alparone, V. Librando, Z. Minniti, *Chem. Phys. Lett.* **2008**, *460*, 151 – 154.
[39] A. Hinchliffe, B. Nikolaidi, H. J. Soscún Machado, *Cent. Eur. J. Chem.* **2005**, *3*, 361 – 369.
[40] A. P. Cox, I. C. Ewart, W. M. Stigliani, *J. Chem. Soc. Faraday Trans. 2* **1975**, *71*, 504 – 514.
[41] R. M. Hochstrasser, L. J. Noe, *Chem. Phys. Lett.* **1970**, *5*, 489 – 492.
[42] R. S. Mulliken, *J. Chem. Phys.* **1955**, *23*, 1833 – 1840.
[43] J. Cioslowski, *J. Am. Chem. Soc.* **1989**, *111*, 8333 – 8336.
[44] A. J. Stone, *The Theory of Intermolecular Forces*, Oxford University Press, Oxford, **2000**.
[45] C. M. Breneman, K. B. Wiberg, *J. Comput. Chem.* **1990**, *11*, 361 – 373.
[46] K. B. Wiberg, P. R. Rablen, *J. Comput. Chem.* **1993**, *14*, 1504 – 1518.
[47] R. H. Michel, *J. Polym. Sci. A Polym. Chem.* **1967**, *5*, 920 – 926.
[48] S. Akiyama, F. Ogura, M. Nakagawa, *Bull. Chem. Soc. Jpn.* **1971**, *44*, 3443 – 3445.
[49] W. Chodkiewicz, P. Cadiot, A. Willemart, *C. R. Hebd. Séances Acad. Sci.* **1957**, *245*, 2061 – 2062.
[50] W. Ried, H. J. Schmidt, K. Wesselborg, *Angew. Chem.* **1958**, *70*, 270 – 270.
[51] J.-H. Lamm, J. Glatthor, J.-H. Weddeling, A. Mix, J. Chmiel, B. Neumann, H.-G. Stammler, N. W. Mitzel, *Org. Biomol. Chem.* **2014**, *12*, 7355 – 7365.
[52] K. Nakasuji, S. Akiyama, K. Akashi, M. Nakagawa, *Bull. Chem. Soc. Jpn.* **1970**, *43*, 3567 – 3576.
[53] Y. Okamoto, K. L. Chellappa, S. K. Kundu, *J. Org. Chem.* **1972**, *37*, 3185 – 3187.
[54] S. Akiyama, M. Nakagawa, *Bull. Chem. Soc. Jpn.* **1970**, *43*, 3561 – 3566.
[55] S. Akiyama, M. Nakagawa, *Bull. Chem. Soc. Jpn.* **1971**, *44*, 2237 – 2248.
[56] J. Sugiyama, I. Tomita, *Eur. J. Org. Chem.* **2007**, 4651 – 4653.
[57] V. A. Korshun, E. V. Manasova, K. V. Balakin, A. D. Malakhov, A. V. Perepelov, T. A. Sokolova, Y. A. Berlin, *Nucleosides Nucleotides* **1998**, *17*, 1809 – 1812.
[58] A. O. King, N. Okukado, E.-i. Negishi, *J. Chem. Soc. Chem. Commun.* **1977**, 683 – 684.
[59] E.-i. Negishi, T. Takahashi, S. Baba, D. E. Van Horn, N. Okukado, *J. Am. Chem. Soc.* **1987**, *109*, 2393 – 2401.
[60] L. Anastasia, E.-i. Negishi, *Org. Lett.* **2001**, *3*, 3111 – 3113.
[61] E.-i. Negishi, L. Anastasia, *Chem. Rev.* **2003**, *103*, 1979 – 2017.
[62] J. A. John, J. M. Tour, *Tetrahedron* **1997**, *53*, 15515 – 15534.
[63] K. Sonogashira, Y. Tohda, N. Hagihara, *Tetrahedron Lett.* **1975**, *16*, 4467 – 4470.
[64] A. Nierth, A. Y. Kobitski, G. U. Nienhaus, A. Jäschke, *J. Am. Chem. Soc.* **2010**, *132*, 2646 – 2654.
[65] M. A. Heuft, S. K. Collins, G. P. A. Yap, A. G. Fallis, *Org. Lett.* **2001**, *3*, 2883 – 2886.
[66] T. N. Hoheisel, H. Frauenrath, *Org. Lett.* **2008**, *10*, 4525 – 4528.
[67] T. N. Hoheisel, H. Frauenrath, *Chimia* **2009**, *63*, 208 – 210.
[68] A. B. Holmes, C. L. D. Jennings-White, A. H. Schulthess, B. Akinde, D. R. M. Walton, *J. Chem. Soc. Chem. Commun.* **1979**, 840 – 842.
[69] A. B. Holmes, G. E. Jones, *Tetrahedron Lett.* **1980**, *21*, 3111 – 3112.
[70] B. Bartik, R. Dembinski, T. Bartik, A. M. Arif, J. A. Gladysz, *New J. Chem.* **1997**, *21*, 739 – 750.
[71] V. Fiandanese, D. Bottalico, G. Marchese, A. Punzi, *Tetrahedron* **2004**, *60*, 11421 – 11425.
[72] V. Fiandanese, D. Bottalico, G. Marchese, A. Punzi, *Tetrahedron* **2006**, *62*, 5126 – 5132.
[73] N. A. Danilkina, A. E. Kulyashova, A. F. Khlebnikov, S. Bräse, I. A. Balova, *J. Org. Chem.* **2014**, *79*, 9018 – 9045.
[74] M. Desroches, M.-A. Courtemanche, G. Rioux, J.-F. Morin, *J. Org. Chem.* **2015**, *80*, 10634 – 10642.
[75] A. S. Hay, *J. Org. Chem.* **1962**, *27*, 3320 – 3321.
[76] H. M. Schmidt, J. F. Arens, *Recl. Trav. Chim. Pays-Bas* **1967**, *86*, 1138 – 1142.
[77] N. D. Marsh, M. J. Wornat, *Poly. Arom. Comp.* **2000**, *19*, 263 – 284.
[78] M. J. Frisch, G. W. Trucks, H. B. Schlegel, G. E. Scuseria, M. A. Robb, J. R. Cheeseman, G. Scalmani, V. Barone, B. Mennucci, G. A. Petersson, H. Nakatsuji, M. Caricato, X. Li, H. P. Hratchian, A. F. Izmaylov, J. Bloino, G. Zheng, J. L. Sonnenberg, M. Hada, M. Ehara, K. Toyota, R. Fukuda, J. Hasegawa, M. Ishida, T. Nakajima, Y. Honda, O. Kitao, H. Nakai, T. Vreven, J. A. Montgomery, Jr., J. E. Peralta, F. Ogliaro, M. Bearpark, J. J. Heyd, E. Brothers, K. N. Kudin, V. N. Staroverov, R. Kobayashi, J. Normand, K. Raghavachari, A. Rendell, J. C. Burant, S. S. Iyengar, J. Tomasi, M. Cossi, N. Rega, J. M. Millam, M. Klene, J. E. Knox, J. B. Cross, V. Bakken, C. Adamo, J. Jaramillo, R. Gomperts, R. E. Stratmann, O. Yazyev, A. J. Austin, R. Cammi, C. Pomelli, J. W. Ochterski, R. L. Martin, K. Morokuma, V. G. Zakrzewski, G. A. Voth, P. Salvador, J. J. Dannenberg, S. Dapprich, A. D. Daniels, O. Farkas, J. B. Foresman, J. V. Ortiz, J. Cioslowski, D. J. Fox, GAUSSIAN 09, Revision A.02, Gaussian, Inc., Wallingford, CT, USA, **2009**.

Received: June 11, 2017
Version of record online July 13, 2017

